Supporting Information

AgX-based hybrid coordination polymers: mechanochemical synthesis, structure and luminescent properties characterization

Caterina Zuffa,[a] Chiara Cappuccino,[b] Marianna Marchini,[a] Laura Contini,[a] Francesco Farinella[a] and Lucia Maini*[a]

1. Knowledge Discovery on Database

ConQuest was used as tool to investigate the Cambridge Structural Database. First, we isolated from the database a subset containing all the structures of interest, namely those compounds that satisfy the following requirements: 1) structures containing silver coordinated simultaneously by X (with X = Cl, Br, I) and L (with L = N, P, As, O, S, Se); 2) structures in which there are no other metals and other semi-metals different form Ag; 3) structures in which the halide is the monoatomic anion; 4) structures without C-Ag bond. In the end, 791 structures met these requirements. We then divided the subset_AgXL into polymeric (*AgXL_Poly*) and non-polymeric structures (*AgXL_NonPoly*). This was done exploiting the *not polymeric* filter provided by the software ConQuest.

Subsequently, in order to facilitate the determination of the coordination number of the halide, we divided each of these two subsets into structures featuring a bridged halide (with coordination number ≥ 2: *AgXL_NonPoly_Xbridge, AgXL_Poly_Xbridge*) and structures that do not have a bridging halide (coordination number of the halide = 1 *AgXL_NonPoly_Xnonbridge, AgXL _Poly_Xnonbridge*). Here we document results of the partition:

Table 1 Partition result of subset_AgXL.

First partition	Structures number	Second partition	Structures number	Third partition	Structures number
Polymeric structures	260	Bridged halide structure	240	Chlorides	87
				Bromides	72
				Iodides	87
		Non-bridged halide structure	20	Chlorides	11
				Bromides	7
				Iodides	2
Non-polymeric structures	531	Bridged halide structure	318	Chlorides	126
				Bromides	108
				Iodides	85
		Non-bridged halide structure	213	Chlorides	118
				Bromides	61
				Iodides	34

To investigate the presence of argentophilic interactions in AgXL we searched for those structures of the *AgXL_subset* that features an Ag-Ag distance of less than 3.44 Å, whether this one distance both intramolecular and intermolecular. Below are reported the results:

Table 2 Structures that satisfy the distance criterion.

Structure typology	Halide position	Halide nature	Total number of structures	Number of structures with argentophilic interactions
Polymeric structures	Bridged halide structure	Chlorides	87	24
		Bromides	72	49
		Iodides	87	75
	Non-bridged halide structure	Chlorides	11	3
		Bromides	7	3
		Iodides	2	0
Non-polymeric structures	Bridged halide structure	Chlorides	126	45
		Bromides	108	59
		Iodides	85	64
	Non-bridged halide structure	Chlorides	118	15
		Bromides	61	2
		Iodides	34	1

2. Crystallographic information

AgI-based coordination polymers

Table 3 Crystal data and structure refinement for $[(AgI)(n\text{-pica})]_n$ coordination polymers.

	$[(AgI)(2\text{-pica})]_n$	**$[(AgI)(3\text{-pica})]_n$**	**$[(AgI)(4\text{-pica})]_n$**
Empirical formula	$C_6H_8AgIN_2$	C_6H_8AgIN2	$C_6H_8AgIN_2$
Formula weight (g mol^{-1})	342.91	342.91	342.91
T (K)	293	293	293
Wavelength (Å)	1.535	0.71073	0.71073
Crystal system	triclinic	monoclinic	monoclinic
Space group	P-1	$P2_1/c$	$P2_1/c$
a (Å)	4.579	16.9162(7)	4.4664(3)
b (Å)	10.323	4.5682(2)	19.2155(11)
c (Å)	10.263	22.7197(8)	10.5788(6)
a (Å)	112.54	90	90
b (Å)	83.86	90.447(4)	96.346(5)
g (Å)	85.59	90	90
V (Å^3)	442	1755(2)	902.35(10)
Z, Z’	2, 1	4, 1	4, 1
ρ_{calc} (mg m^{-3})	2.577	2.595	2.524
μ (mm^{-1})		5.743	5.587
F(000)		1264	632
crystal size (mm)	powder	0.4028×0.0774×0.0618	0.05×0.04×0.03
ϑ range for data collection (◦)	5° to 70°	3.587° to 29.528°	3.725° to 29.290°
reflections collected		9734	3158
Independent reflections		4082	1891
R_{int}	0.0063	0.0939	0.0236
Completeness to theta = 25.000°		99.8%	96.7%
Refinement method	Rietveld	Full-matrix least-squares on F^2	Full-matrix least-squares on F^2
T_{max}/T_{min}		1.00000/0.25756	1.00000/0.80811
data/restraints/parameters		4082 / 0 / 181	1891 / 0 / 99
Goodness-of-fit	2.036	1.065	1.051
R1 [I > 2σ(I)]	0.0280	0.0596	0.0486
*w*R2 (all data)	0.0370	0.1351	0.0837

AgBr-based coordination polymers

Table 4 Crystal data and structure refinement for $[(AgBr)(n\text{-pica})]_n$ coordination polymers.

	$[(AgBr)(2\text{-pica})]_n$	**$[(AgBr)(3\text{-pica})]_n$**	**$[(AgBr)(4\text{-pica})]_n$**
Empirical formula	$C_6H_8AgBrN_2$	$C_6H_8AgBrN_2$	$C_6H_8AgBrN_2$
Formula weight (g mol^{-1})	295.915	295.915	295.915
T (K)	293	293	293
Wavelength (Å)	0.71073	0.71073	1.535
Crystal system	triclinic	monoclinic	monoclinic
Space group	P-1	$P2_1/c$	$P2_1/c$
a (Å)	4.3871(5)	9.4518(6)	6.316
b (Å)	10.1081(12)	6.1880(3)	7.365
c (Å)	10.2510(18)	14.3981(9)	17.769
a (Å)	113.498(14)	90	90
b (Å)	97.081(12)	105.712(6)	81.08
g (Å)	93.535(9)	90	90
V (Å^3)	410.63(11)	810.64(8)	816
Z, Z’	2, 1	4, 1	4, 1
ρ_{calc} (mg m^{-3})	2.393	2.425	2.407
μ (mm^{-1})	7.244	7.339	
F(000)	280	560	
crystal size (mm)	0.379×0.201×0.039	0.141×0.134×0.041	powder
ϑ range for data collection (◦)	3.704° to 29.105°	3.606° to 29.112°	5° to 60°
reflections collected	3052	3457	

Independent reflections	1853	1874	
R_{int}	0.0253	0.0307	0.0143
Completeness to theta = 25.000°	99.7%	99.8%	
Refinement method	Full-matrix least-squares on F^2	Full-matrix least-squares on F^2	Rietveld
T_{max}/T_{min}	1.00000/0.67900	1.00000/0.45264	
data/restraints/parameters	1853 / 0 / 92	1874 / 0 / 91	
Goodness-of-fit	0.983	1.041	1.337
R1 [I > 2σ(I)]	0.0448	0.0419	0.0290
*w*R2 (all data)	0.0854	0.0852	0.0369

3. PXRD pattern

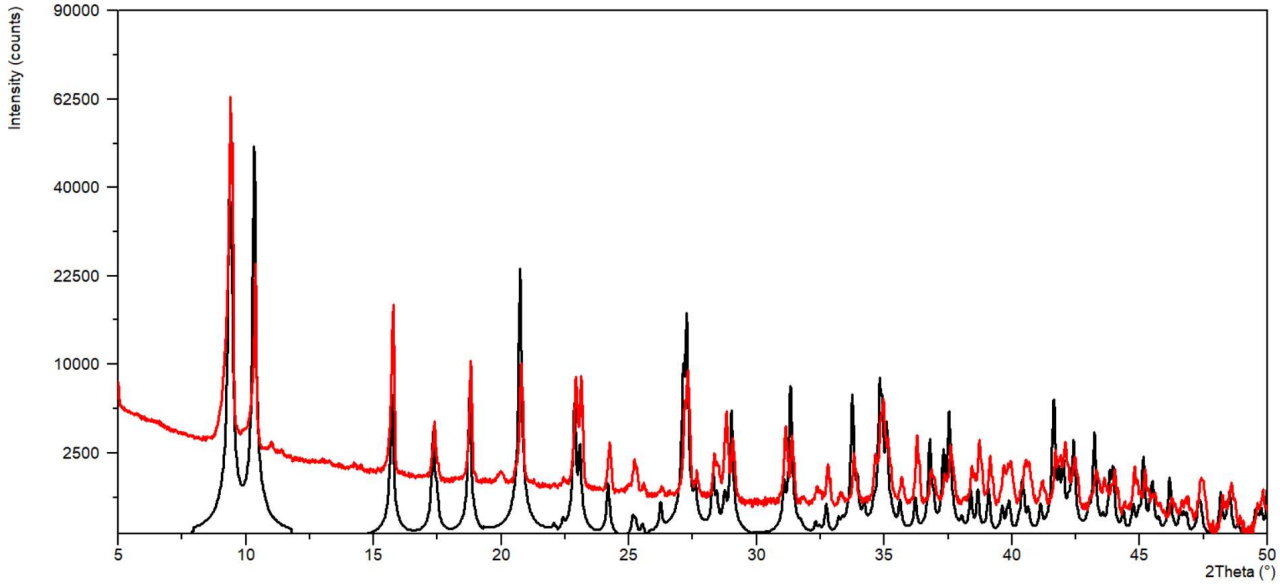

Figure 1 Comparison between calculated (black line) and experimental (red line) X-ray powder diffraction patterns of $[(AgI)(2\text{-pica})]_n$. The diffractograms are shown in square root intensity mode. Peaks at 2θ = 22.43° and 25.20° belong to AgI.

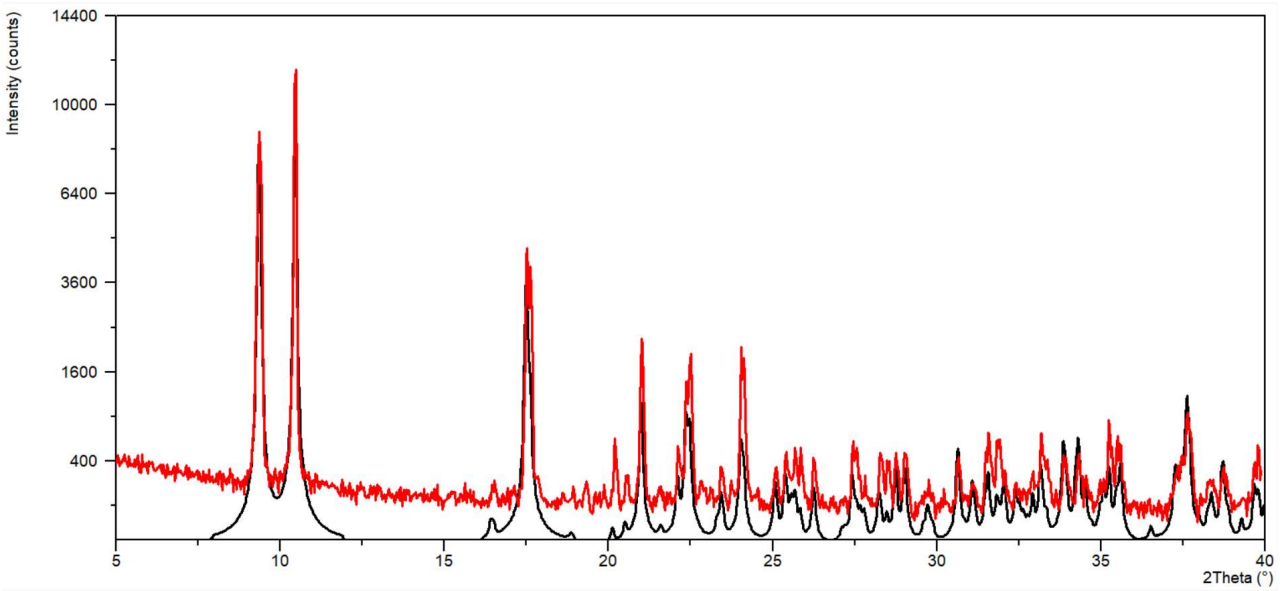

Figure 2 Comparison between calculated (black line) and experimental (red line) X-ray powder diffraction patterns of $[(AgI)(3\text{-pica})]_n$. The diffractograms are shown in square root intensity mode.

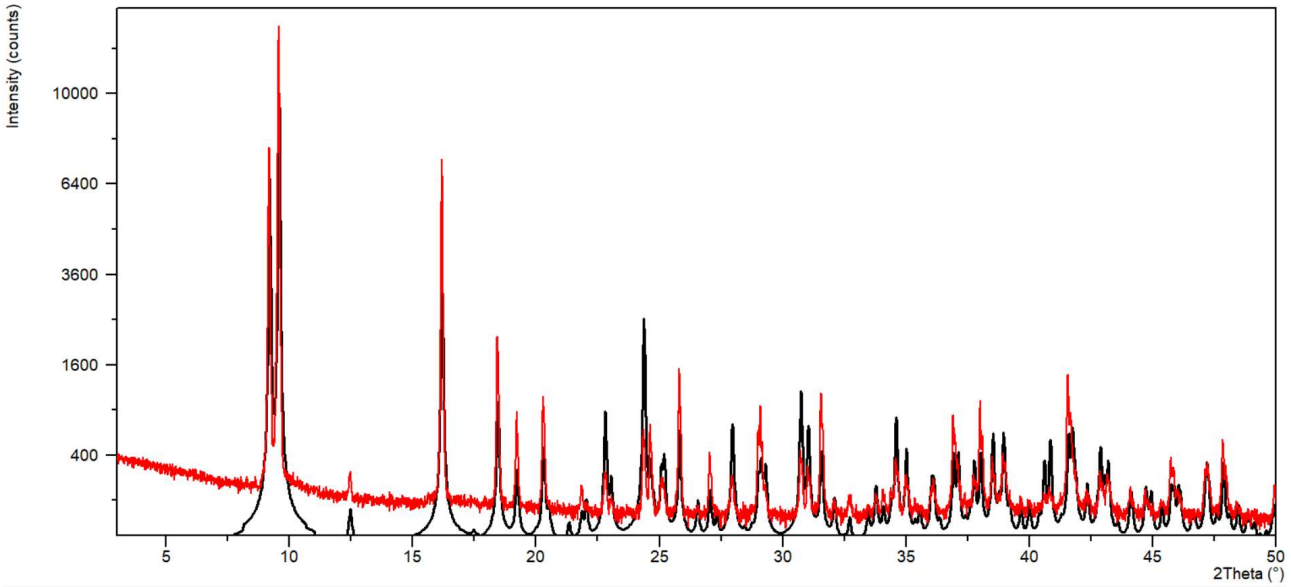

Figure 3 Comparison between calculated (black line) and experimental (red line) X-ray powder diffraction patterns of $[(AgI)(4\text{-pica})]_n$. The diffractograms are shown in square root intensity mode.

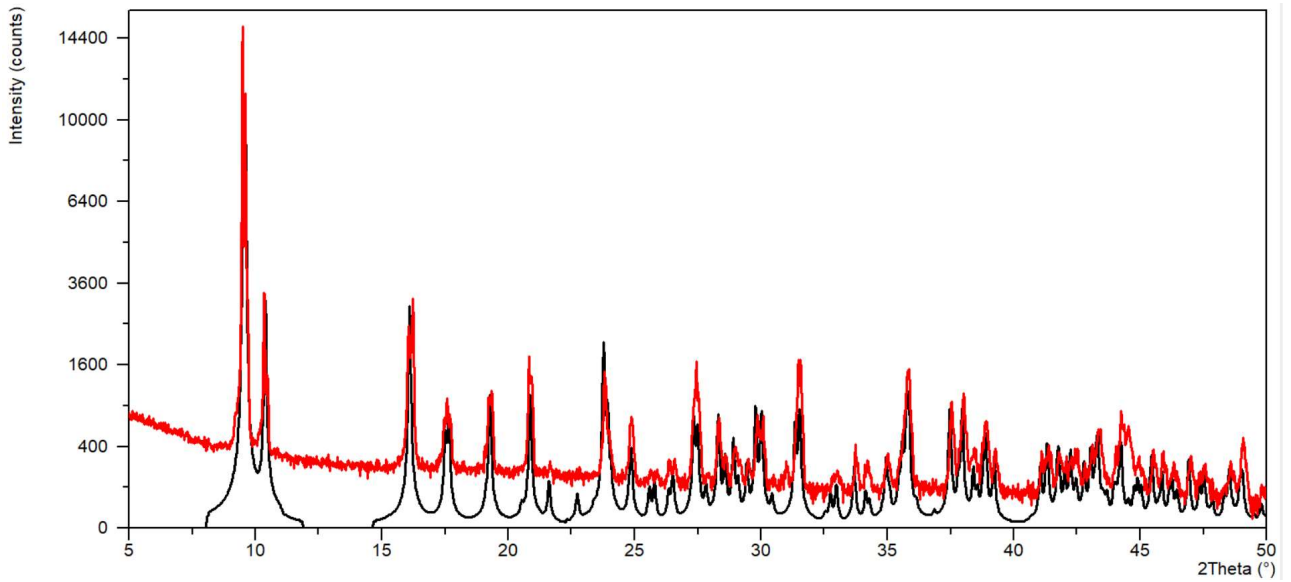

Figure 4 Comparison between calculated (black line) and experimental (red line) X-ray powder diffraction patterns of $[(AgBr)(2\text{-pica})]_n$. The diffractograms are shown in square root intensity mode.

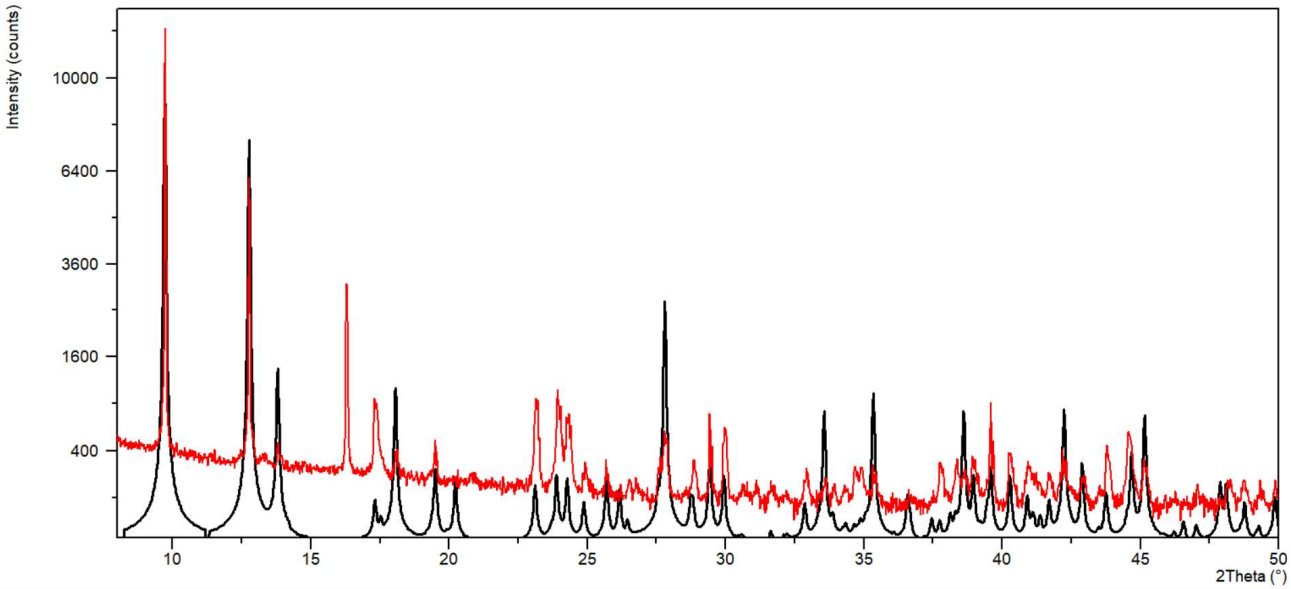

Figure 5 Comparison between calculated (black line) and experimental (red line) X-ray powder diffraction patterns of $[(AgBr)(3\text{-pica})]_n$. The diffractograms are shown in square root intensity mode. The peak at $2\theta = 16.30°$ belongs to the sample holder.

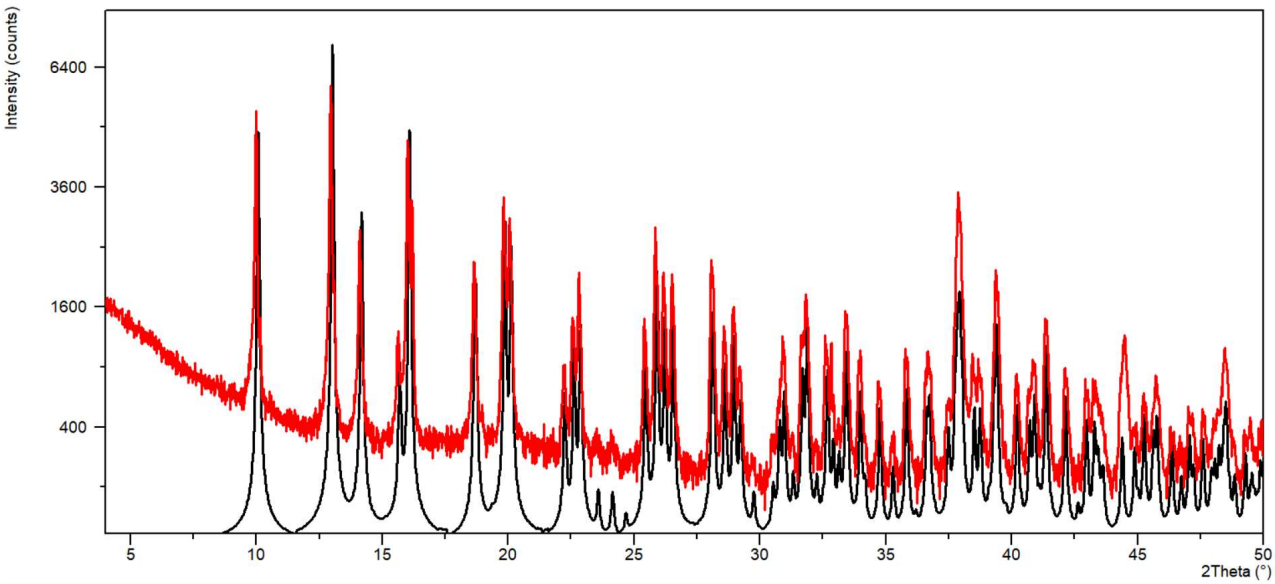

Figure 6 Comparison between calculated (black line) and experimental (red line) X-ray powder diffraction patterns of $[(AgBr)(4\text{-pica})]_n$.

3. Rietveld refinement

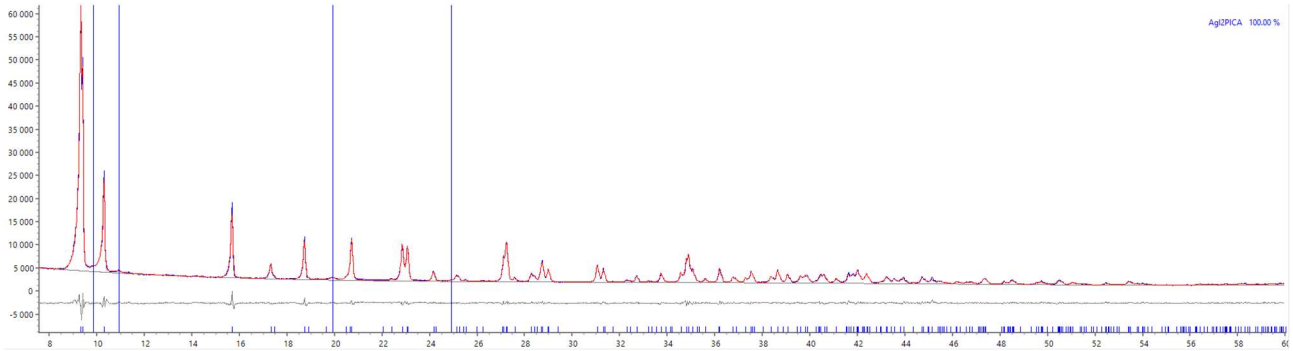

Figure 7 Rietveld refinement (red line) on [(AgI)(2-pica)]n diffraction pattern (blue line). The blue lines indicate weak and broad peaks due to impurities. In grey, the difference plot.

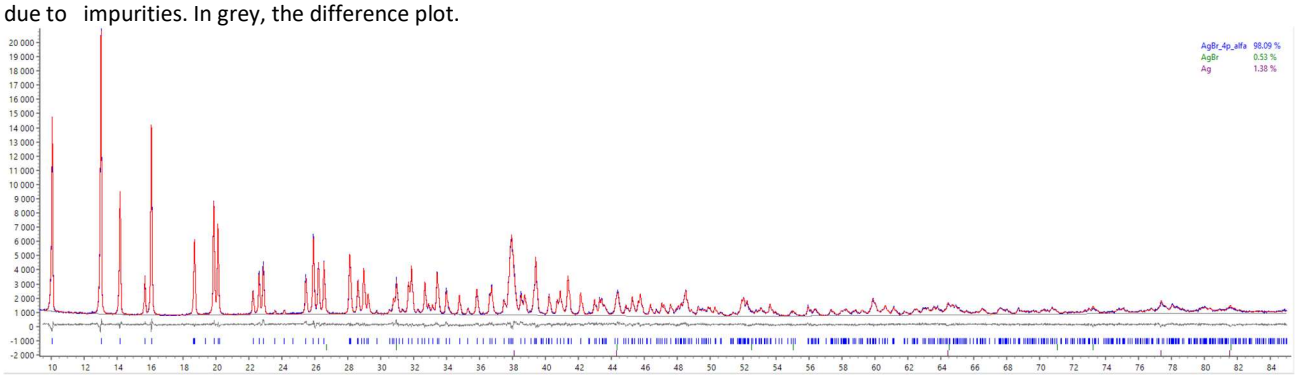

Figure 8 Rietveld refinement (red line) on [(AgBr)(4-pica)]n diffraction pattern (blue line). Peaks of unreacted AgBr and Ag (due to photodecomposition) are present. In grey, the difference plot.

4. Luminescence properties

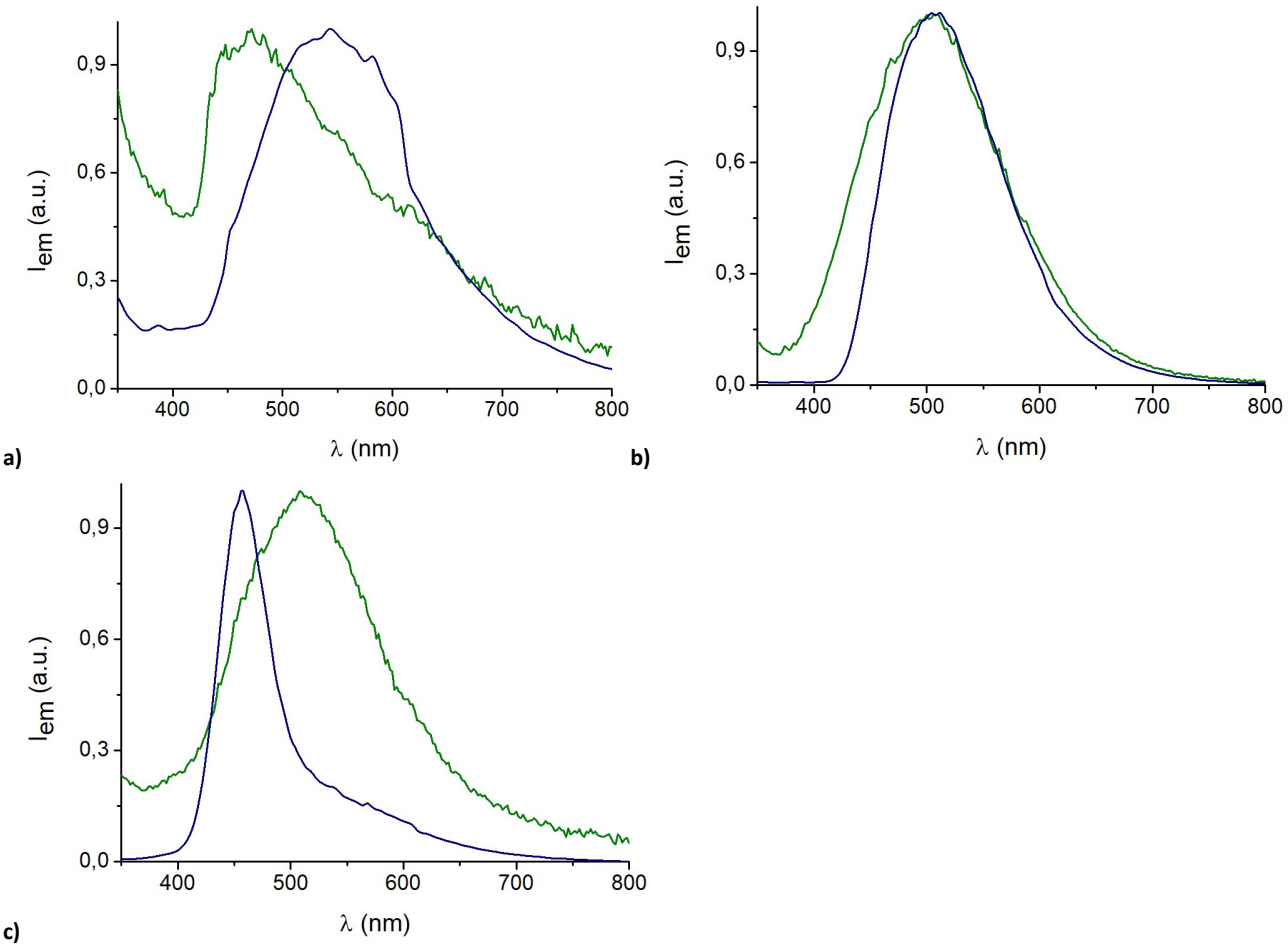

Figure 9 Solid state emission spectra at room temperature (green line) and at 77K (blue line) of **a)** $[(AgBr)(2\text{-pica})]_n$; **b)** $[(AgBr)(3\text{-pica})]_n$; **c)** $[(AgBr)(4\text{-pica})]_n$ obtained by ball milling.

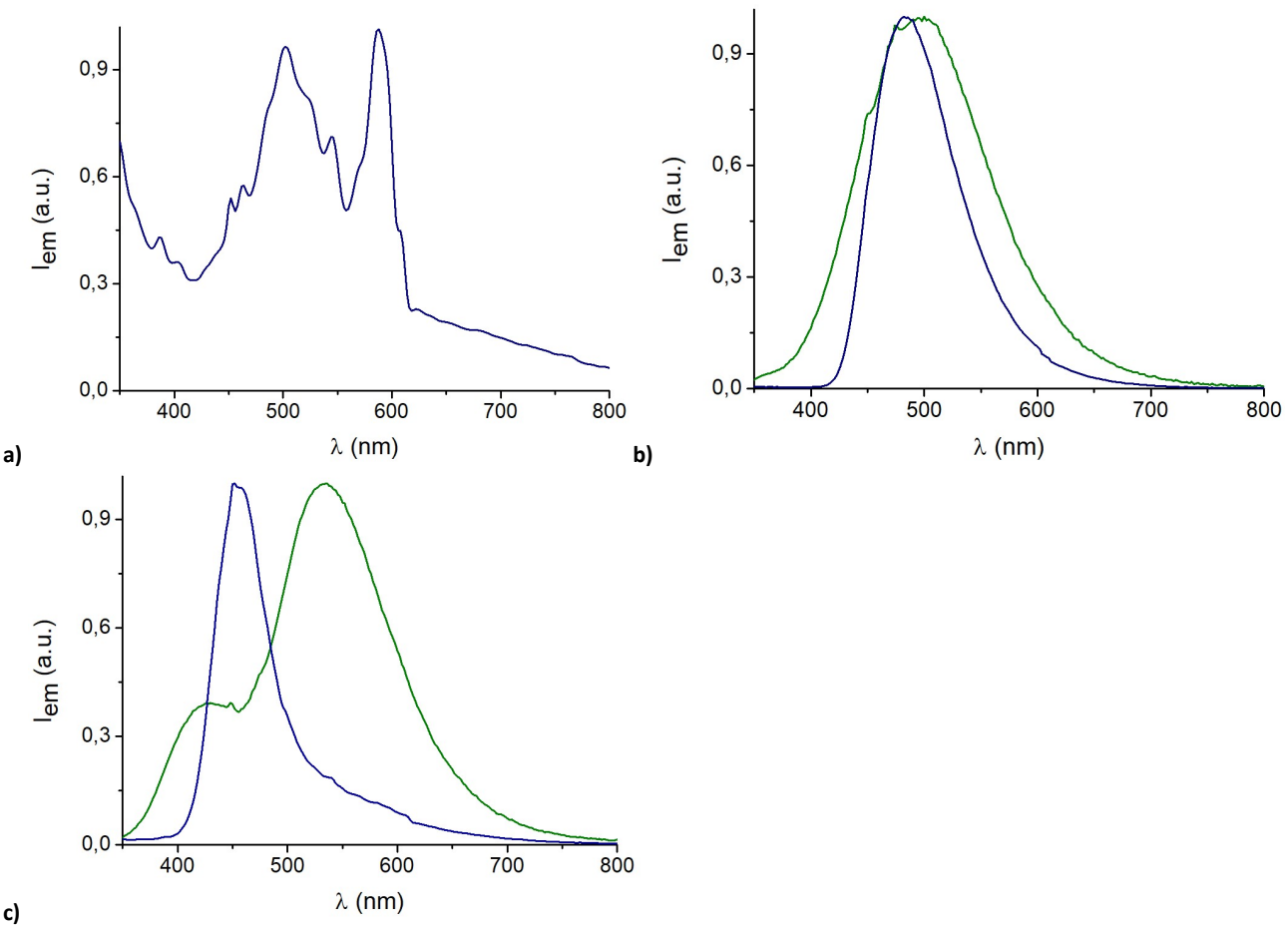

Figure 10 Solid state emission spectra at room temperature (green line) and at 77K (blue line) of **a)** $[(AgBr)(2\text{-pica})]_n$; **b)** $[(AgBr)(3\text{-pica})]_n$; **c)** $[(AgBr)(4\text{-pica})]_n$ obtained by slurry.

4. TGA analysis

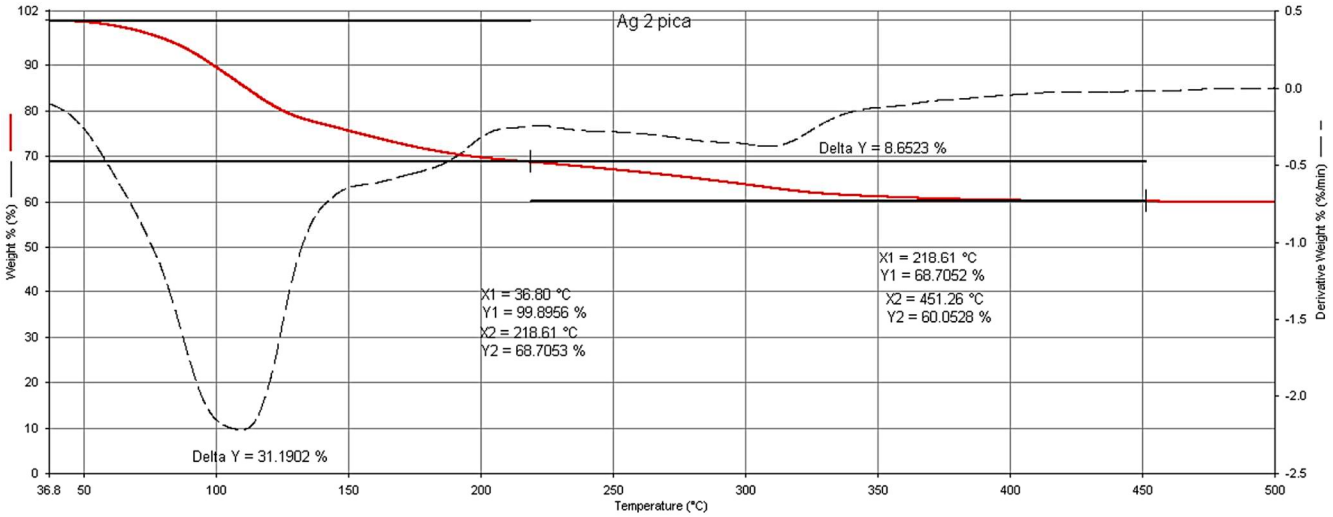

Figure 11 TGA analysis of $[(AgI)(2\text{-pica})]_n$.

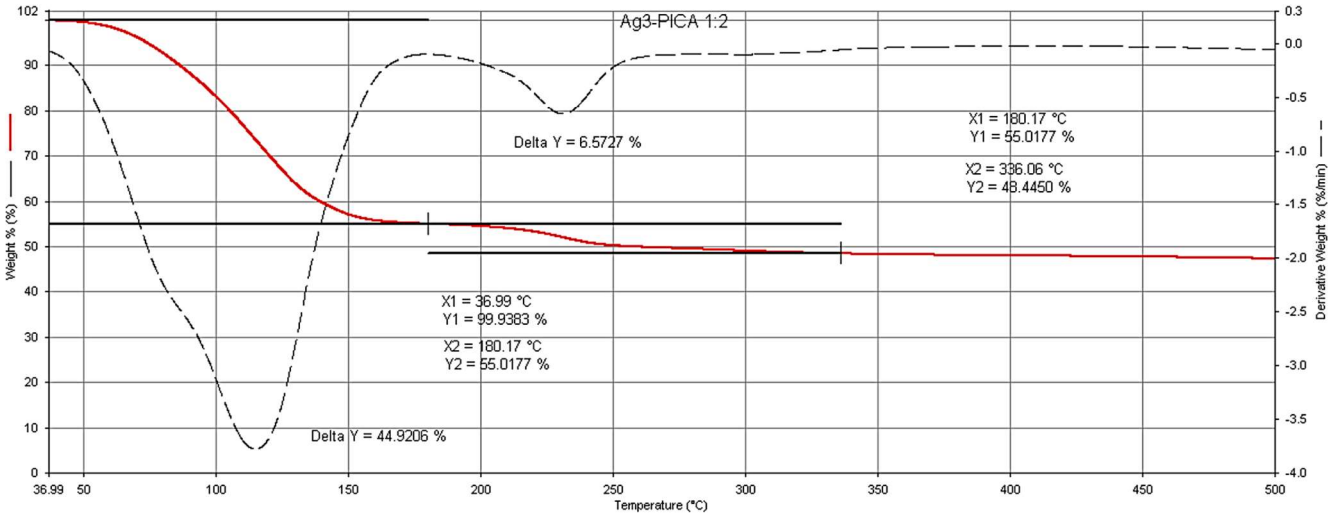

Figure 12 TGA analysis of $[(AgI)(3\text{-pica})]_n$.

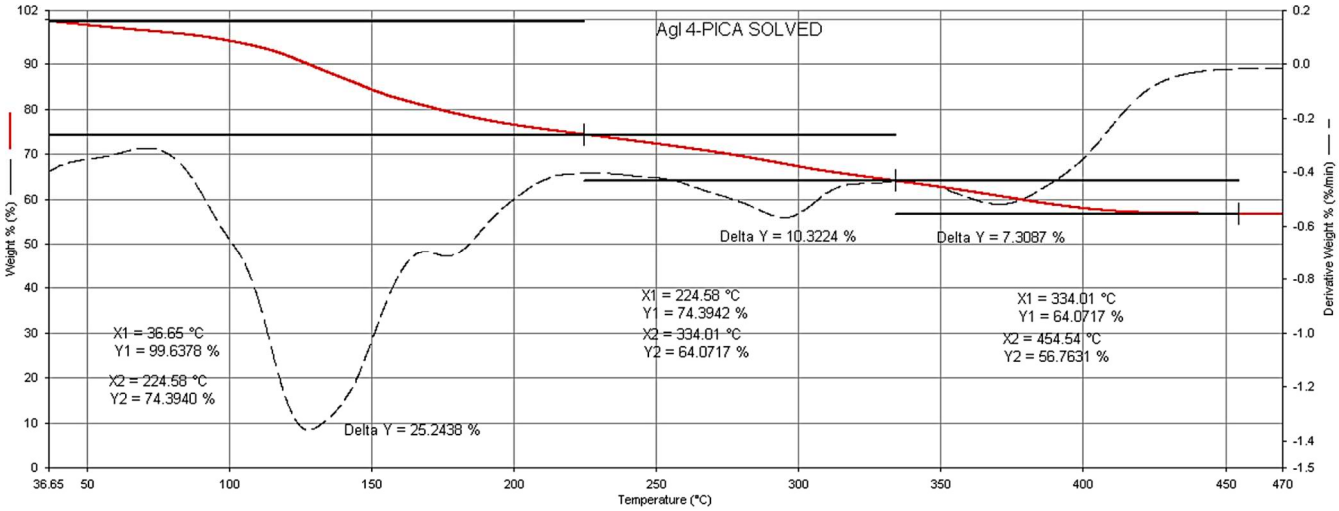

Figure 13 TGA analysis of $[(AgI)(4\text{-pica})]_n$.

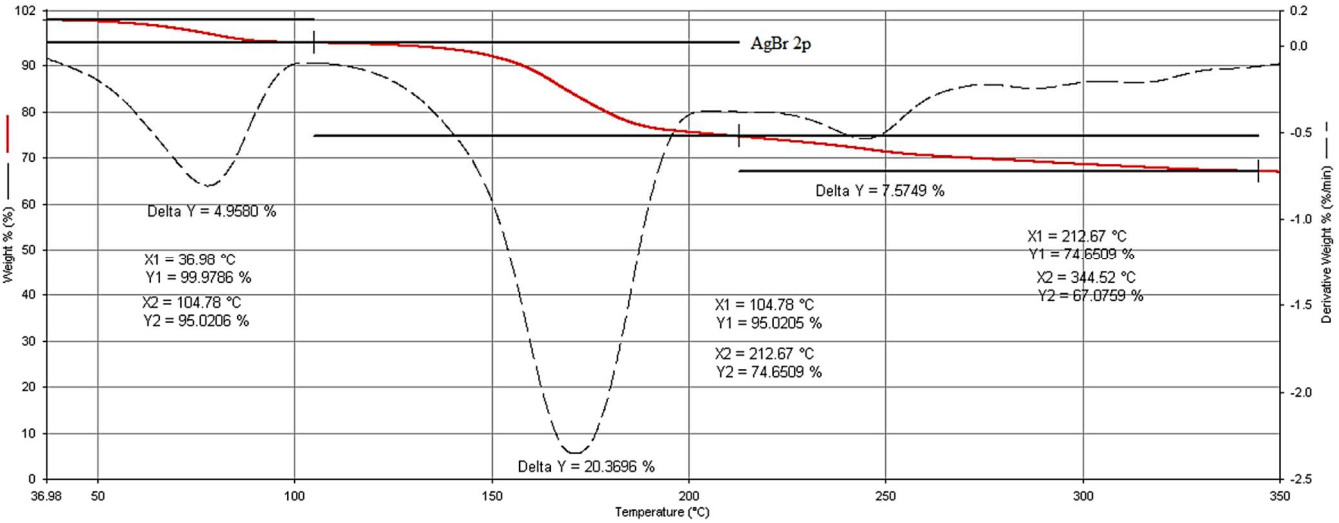

Figure 14 TGA analysis of $[(AgBr)(2\text{-pica})]_n$.

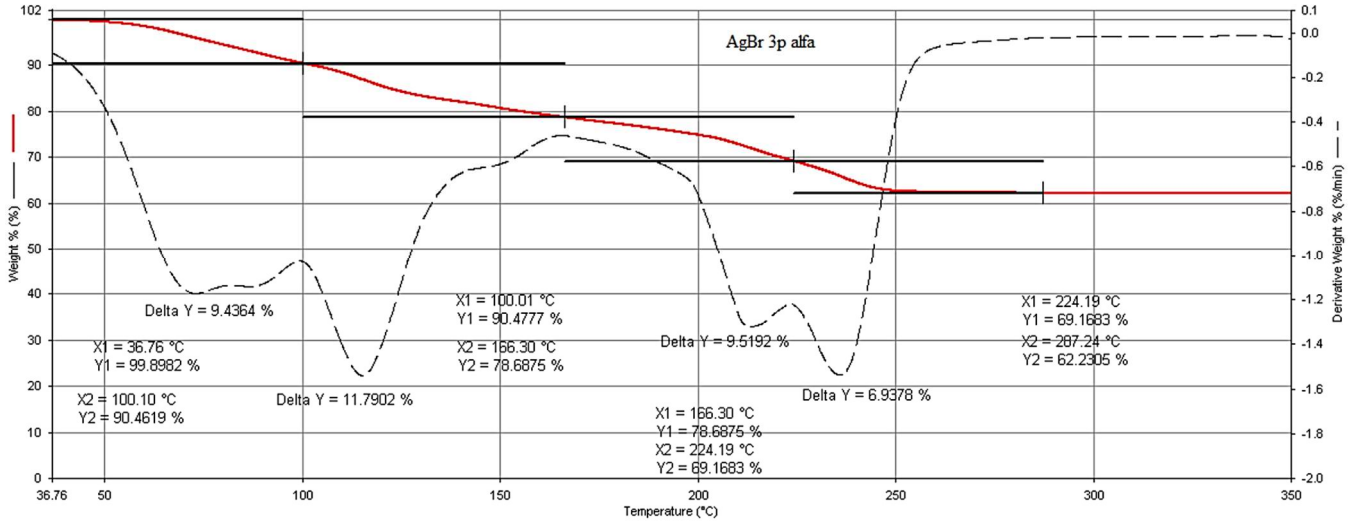

Figure 15 TGA analysis of $[(AgBr)(3\text{-pica})]_n$.

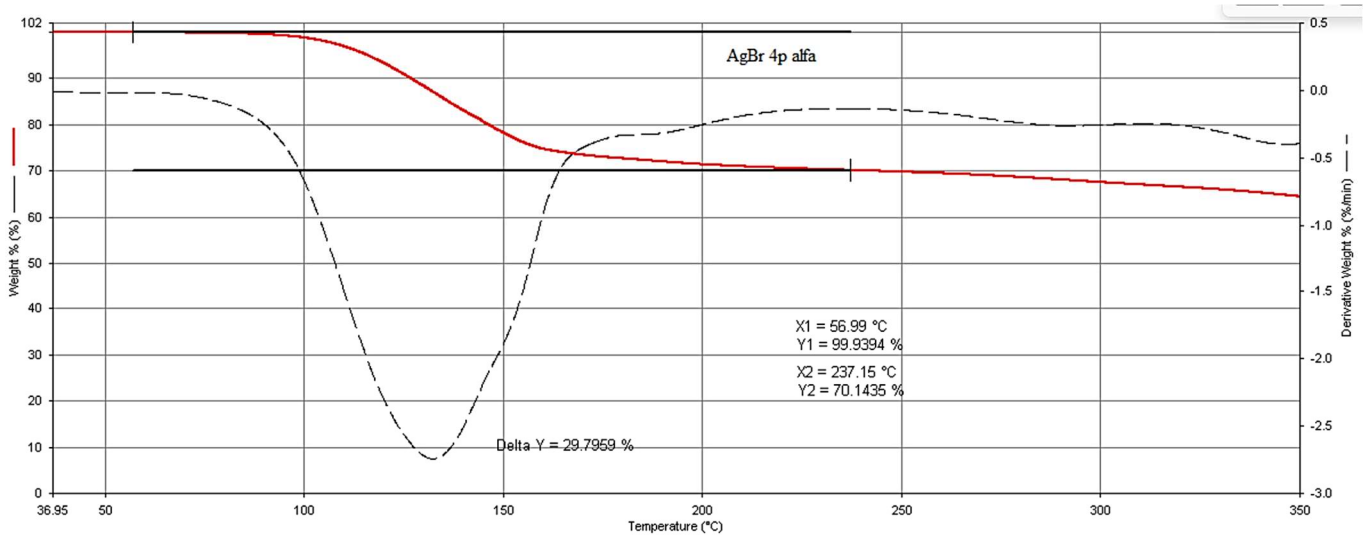

Figure 16 TGA analysis of $[(AgBr)(4\text{-pica})]_n$.

5. 4-pica$^+$Br$^-$

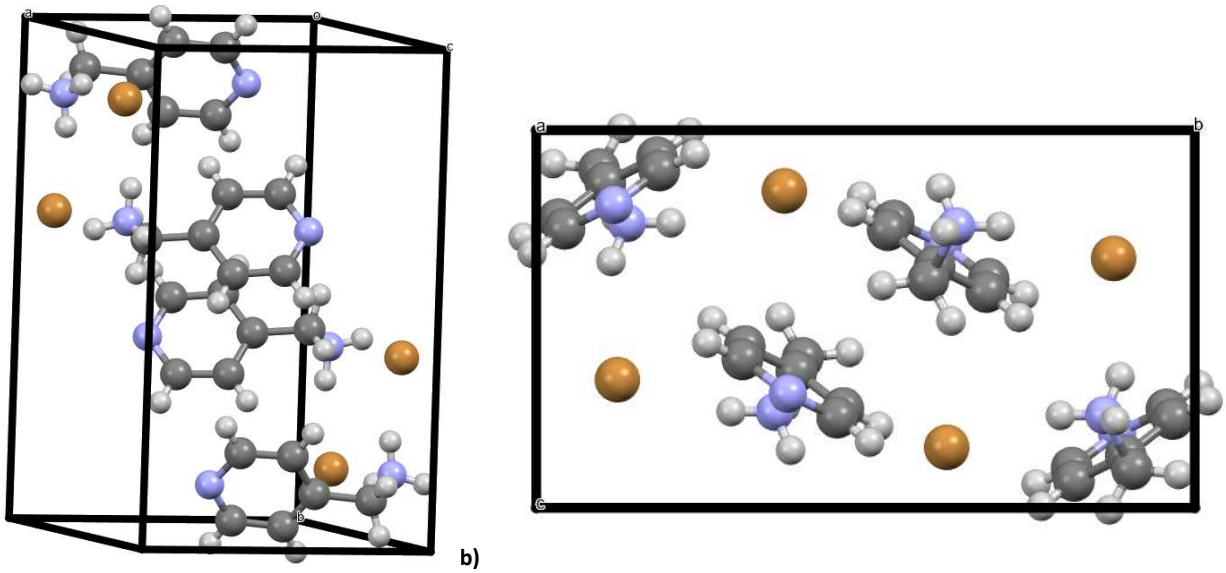

a) **b)**

Figure 17 a) 4-pica$^+$Br$^-$ structure; **b)** packing along a-axis.

	4-pica$^+$Br$^-$
Empirical formula	$C_6H_9N_2Br$
Formula weight (g mol^{-1})	252.08
T (K)	293
Wavelength (Å)	0.71073
Crystal system	monoclinic
Space group	$P2_1/c$
a (Å)	7.8259(5)
b (Å)	13.3434(7)
c (Å)	7.8729(8)
a (Å)	90
b (Å)	103.640(9)
g (Å)	90
V (Å^3)	798.934
Z, Z'	4, 1
ρ_{calc} (mg m^{-3})	1.572
μ (mm^{-1})	5.064
F(000)	376
crystal size (mm)	0.475×0.364×0.021
ϑ range for data collection (◦)	3.638° to 28.967°
reflections collected	2231
Independent reflections	1427
R_{int}	0.0293
Completeness to theta = 25.000°	99.8%
Refinement method	Full-matrix least-squares on F^2
T_{max}/T_{min}	1.00000/0.65876
data/restraints/parameters	1427 / 0 / 83
Goodness-of-fit	1.069
R1 [I > 2σ(I)]	0.0428
*w*R2 (all data)	0.0913

CCDC 2170412 contains the supplementary crystallographic data for this paper. The data can be obtained free of charge from The Cambridge Crystallographic Data Centre via www.ccdc.cam.ac.uk/structures.